ELSEVIER

Coordination Chemistry Reviews
190–192 (1999) 707–735

COORDINATION CHEMISTRY REVIEWS

www.elsevier.com/locate/ccr

Low temperature route towards new materials: solvothermal synthesis of metal chalcogenides in ethylenediamine

Jing Li [a,*], Zhen Chen [a], Ru-Ji Wang [a], Davide M. Proserpio [b]

[a] *Department of Chemistry, Rutgers University, Camden, NJ 08102, USA*
[b] *Dipartimento di Chimica Strutturale e Stereochimica Inorganica Universita di Milano, 20133 Milan, Italy*

Received 24 November 1998; accepted 13 March 1999

Contents

* Corresponding author. Fax: +1-609-2256160.
E-mail address: jingli@crab.rutgers.edu (J. Li)

0010-8545/99/$ - see front matter © 1999 Elsevier Science S.A. All rights reserved.
PII: S0010-8545(99)00107-1

Abstract

Solid state reactions occur among solid reactants and are characterized by slow nucleation and diffusion processes. Thus, high temperature is often required to promote the reactions to proceed at an appropriate rate. Kinetic control and mechanistic study of these systems are usually very difficult. One has little control in rational design and prediction of the structures coming out of the reactions. High temperature products are often limited to the thermodynamically most stable phases. The recent development in soft synthesis of metal chalcogenides has been motivated and stimulated by the tremendous progress in the crystal engineering of organic and coordination compounds via molecular building-block approaches. The hope is that by turning down the temperature, the solid state synthesis may proceed in a more controlled and predictable manner. Much research has been carried out in exploration and investigation of various soft synthetic techniques. In this article, we will focus only on the recent development in solvothermal synthesis using ethylenediamine as a reaction medium. © 1999 Elsevier Science S.A. All rights reserved.

Keywords: Solvothermal synthesis; Ethylenediamine; Metal chalcogenides; Chalcogenidometalates

1. Introduction

Hydrothermal synthesis [1] involves use of water as a solvent at elevated temperatures and pressures in a closed system, often in the vicinity of its critical point. A more general term 'solvothermal' refers to a similar reaction in which a different solvent (organic or inorganic) is used. Under hydro(solvo)thermal conditions, certain properties of the solvent, such as density, viscosity and diffusion coefficient change dramatically and the solvent behaves much differently from what is expected at ambient conditions [1d]. Consequently, the solubility, the diffusion process and the chemical reactivity of the reactants (usually solids) are greatly

increased or enhanced. This enables the reaction to take place at a much lower temperature. The method has been widely applied and well adopted for crystal growth of many inorganic materials, such as zeolites, quartz, metal carbonates, phosphates and other oxides and halides [2].

The recent extensive investigations on solvothermal synthesis of metal chalcogenides (sulfides, selenides and tellurides) have been motivated largely by the potential of this method to generate new materials that have specified and desired structures and properties. Unlike most other solid state synthetic techniques, solvothermal synthesis concerns a much milder and softer chemistry conducted at low temperatures. The mild and soft conditions make it possible to leave polychalcogen building-blocks intact while they reorganize themselves to form various new structures, many of which might be promising for applications in catalysis, electronic, magnetic, optical and thermalelectronic devices [3], and to allow formation and isolation of phases that may not be accessible at higher temperatures due to their metastable nature [4].

Much of the work so far has focused on reactions in water and alcohol. Pioneer contributions were made by Schäfer and Sheldrick and their co-workers, who synthesized a number of alkali metal and alkaline-earth metal and group 14–15 sulfides and selenides in superheated water (120–220°C) [5,6], Numerous other metal based chalcogenides were later isolated by Kanatzidis et al. [7,8]. The methanothermal reactions are usually conducted in the temperature range of 110–200°C and have afforded a number of chalcogen rich alkali-metal polychalcogenides [9] and main group chalcogenides [10,11]. A comprehensive review on these systems has been given by Sheldrick and Wachhold [4b].

Ammines (and their cations) are commonly used as organic templates. They act as structure directing agents [1b] during the crystallization processes. Recent developments in the incorporation of such template molecules or ions into inorganic frameworks have resulted in a number of chalcogenide-based open-framework structures [12–14]. Reactions using amines as solvent, however, are comparably unexplored and quite limited [15]. Early work by Jacobs and Schmidt performed in ammonothermal solutions dealt with rather high temperatures (≥ 500°C) and pressures (≥ 6 kbar) [16]. Kolis et al. have subsequently investigated some sulfide and selenide systems under relatively milder conditions. They have prepared a number of monovalent transition metal compounds in superheated ethylenediamine (critical temperature and pressure: $T_c = 319.9$°C, $P_c = 62.1$ atm [17]) at 300–350°C [18–21]. Crystallization of chalcogenides in ethylenediamine [22] and ammonia ($T_c = 132.4$°C, $P_c = 111.3$ atm) [23–25] solutions at even lower temperatures (160–170°C) has only been reported recently. New compounds with a variety of structure types have been discovered via this route [22–40]. This paper will focus primarily on our recent development in soft solvothermal synthesis ($T < 200$ °C) using ethylenediamine as a reaction medium.

Table 1
Physical constants for ethylenediamine

Molecular formula	$C_2H_8N_2$	Formula weight (FW/g·mol^{-1})	60.10
Melting point (T_m/°C)	8.5	Density (d/g·cm^{-3})	0.8977_4^{20}
Boiling point (T_b/°C)	117.3	Refractive index	1.4568^{20}
Flash point (T_f/°C)	43	Viscosity (η/mN·s·m^{-2})	1.54 (20°C)
Critical temp. (T_c/°C)	319.9	Dielectric constant (ε)	14.2 (20°C)
Critical pressure (P_c/atm)	62.1	Dipole moment (μ/D)	1.96 (25°C, g [a])
Critical volume (V/cm^3 mol^{-1})	206	Solubility	misc-w, al [b]; i-bz

[a] Gas.
[b] Misc = miscible, w = water, al = ethanol, i = insoluble, bz = benzene.

2. Synthesis

2.1. The solvent

Ethylenediamine ($H_2NCH_2CH_2NH_2$), also called 1,2-ethanediamine, is an excellent solvent for solvothermal synthesis of metal chalcogenides. Table 1 lists some physical constants of this chemical species [17]. The relatively low critical pressure makes it possible to conduct many reactions in thick-walled glass tubes under mild temperature conditions (e.g. $T < 180$°C). This greatly simplifies the reaction procedure and is more effective in a number of ways compared to reactions in a high pressure reactor. Many inorganic species have reasonable solubility in en, such as alkali-metal chalcogenides (e.g. A_2Q, A = K, Rb, Cs; Q = S, Se, Te) and metal chlorides, which are common reagents used in the solvothermal synthesis of metal chalcogenides. The estimated solubility of selected A_2Q (A = K, Rb, Cs; Q = Se, Te) and M_xCl_y species are given in Tables 2 and 3.

2.2. The reaction vessels

Depending on the reaction temperature and pressure, synthesis may be carried out in (a) a glass ampoule; (b) an acid digestion bomb, or (c) a high-pressure autoclave. For reactions in ethylenediamine below 180°C, a thick-wall Pyrex glass

Table 2
Estimated solubility of A_2Q (A = K, Rb, Cs; Q = Se, Te) in ethylenediamine (25°C, 1 atm)

Sample	Solution color	FW	Solubility/g·l^{-1}	Solubility/10^3 mol·l^{-1}
K_2Se	Yellow	157.92	0.35	2.2
Rb_2Se	Yellow	249.9	0.31	1.3
Cs_2Se	Yellow	344.8	0.45	1.3
K_2Te	Purple	205.8	0.21	1.0
Rb_2Te	Purple	298.5	0.23	0.8
Cs_2Te	Purple	393.4	<0.77	<0.43

Table 3
Estimated solubility of selected metal chlorides in ethylenediamine (25°C, 1 atm)

Sample	Solution color	FW	Solubility/g·l^{-1}	Solubility/10^3 mol·l^{-1}
$MnCl_2$	Yellow	125.84	0.15	1.2
$FeCl_2$	Yellow	126.75	0.12	0.90
$FeCl_3$	Brown	162.2	0.17	1.1
$CoCl_2$	Yellow	129.83	0.22	1.7
$NiCl_2$	Violet	129.61	0.11	0.85
$PdCl_2$	Colorless	177.3	<0.10	<0.56
CuCl	Blue	98.99	0.46	4.6
$CuCl{\cdot}2H_2O$	Blue	170.44	0.30	1.7
Hg_2Cl_2	Colorless	472.1	0.29	0.62
$HgCl_2$	Light yellow	271.5	0.32	1.2
$ZnCl_2$	Colorless	136.27	<0.11	<0.80
$CdCl_2$	Colorless	183.3	<0.11	<0.60
$InCl_3$	Colorless	221.15	0.53	2.4
$SnCl_2$	Yellow	189.6	<0.15	<0.79
$SbCl_3$	Colorless	228.15	<0.15	<0.66
$BiCl_3$	Colorless	315.35	<0.14	<0.44

tube with approx. 9 mm of OD and 5–6 inch of length is usually sufficient to withstand the pressure exerted by the solvent ($\sim$0.35–0.4 ml). The top portion of Fig. 1 shows several Pyrex tubes loaded with samples. A general purpose bomb may be suitable for reactions carried out at higher temperatures (180–250°C). It typically consists of a cylindrical body (stainless steel), a screw cap and a Teflon liner with cover. The lower portion of Fig. 1 displays a Parr 23 ml acid digestion bomb that is commonly used in hydrothermal experiments. For reactions at even higher temperature and pressure, a high-pressure autoclave may be employed.

2.3. The reagents

Metal chlorides have been used in all reactions as a source of metal ions. As shown in Table 3, many of them are relatively soluble in ethylenediamine. In some reactions, the chloride ion (Cl^-) also functions as a mineralizer [1d]. In fact, like carbonate ion CO_3^{2-}, it is known as one of the most common mineralizers for the formation of natural crystals. A_2Q/nQ are often used as sources of polychalcogen anions and alkali-metal counter ions. A number of binary metal chalcogenides such as Sb_2Se_3 and SnQ (Q = Se, Te) have also been used in some reactions.

2.4. The solvothermal reactions

Most of the solvothermal reactions in ethylenediamine involve an oxidation-reduction process. Depending on the reagents used in the synthesis, such a process may be classified into different types. In the first type of reaction, the metal ions (M^{+n}) that form direct bonds to chalcogens are oxidized while the chalcogens are

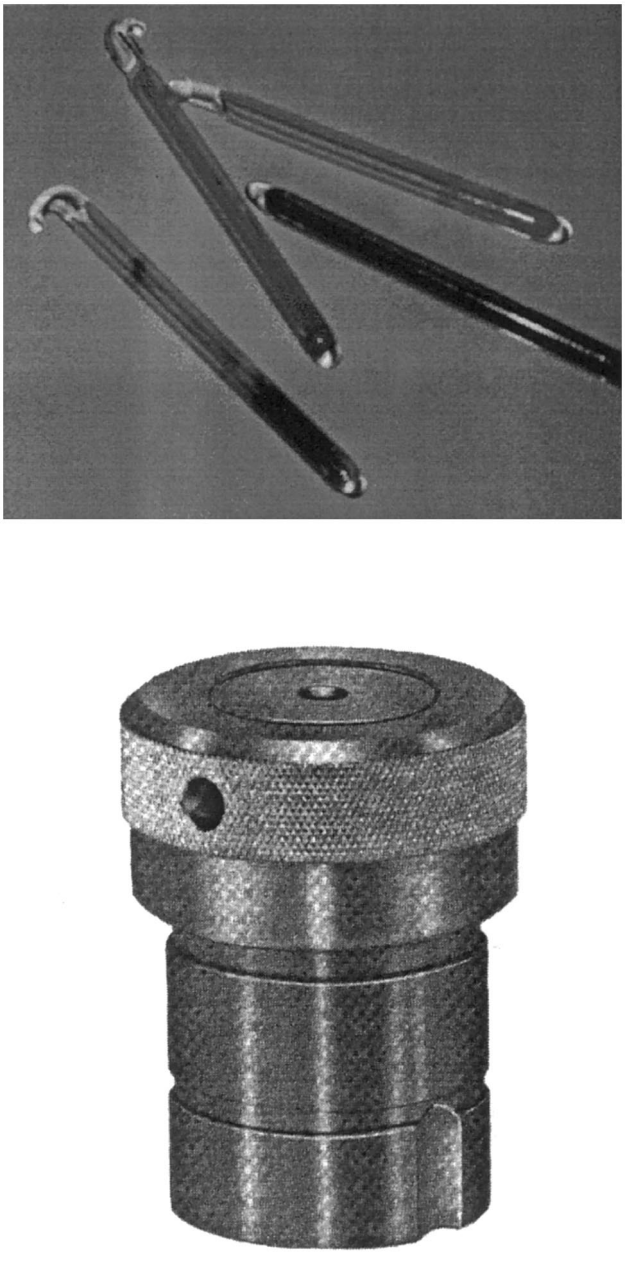

Fig. 1. Reaction vessels commonly used in solvothermal reactions. Top: loaded and sealed thick-wall Pyrex ampoules; Bottom: a Parr 23 ml acid digestion bomb.

reduced. This has been observed in reactions involving Hg_2Cl_2, $SnCl_2$/SnQ and $SbCl_3$, as in the formation of $[M(en)_3]Hg_2Te_9$, M = Mn [28], Fe [22], $Rb_2Hg_3Te_4$ [27], $\{[M(en)_3]_2Cl_2\}Hg_2Te_4$ [28], $[Fe(en)_3](enH)SbSe_4$ [35], $AHgSbQ_3$ (A = Rb, Cs, Q = Se [37b] and A = Rb, Q = Te [29]), $Rb_2Hg_6Se_7$ [38]; $[M(en)_3]Sn_2Q_6$, M = Mn, Zn, Q = Se, Te [32,33], $[Mn(en)_3]CdSnTe_4$ and $[Mn(en)_3]Ag_6Sn_2Te_8$ [39]:

$$Hg_2^{+} \rightarrow 2Hg^{2+} \text{ or } Sn^{2+} \rightarrow Sn^{4+} \text{ or } Sb^{3+} \rightarrow Sb^{5+}$$

$$nQ \rightarrow Q_m^{2-} \quad (m \leq n)$$

In the second type of reaction, the oxidation state of the metal ions remains the same, while the chalcogens undergo a disproportionation process, as in the cases of $[M(en)_3]In_2Te_6$ (M = Fe, Zn) [26], Cs_2PdSe_8 [37a] and $[Ga(en)_3]In_3Te_7$ [40]:

$$nQ \rightarrow Q_m^{2-} \quad (m \leq n)$$

$$n'Q^{2-} \rightarrow Q_{m'}^{2-} \quad (m' \leq n')$$

A number of divalent metal ions, including Mn^{2+}, Fe^{2+}, Co^{2+}, Ni^{2+} and Zn^{2+}, have shown strong coordination ability towards the solvent molecules. Reactions involving these ions in en solution often result in complex cations such as $[M(en)_3]^{2+}$ in which three en molecules chelate to the metal center (M) to give an octahedral geometry. The complex cation so formed usually act as a template and incorporate into the final products:

$$MCl_2 + 3en \rightarrow [M(en)_3]^{2+} + 2Cl^{-}$$

$$[M(en)_3]^{2+} + (M'_xQ_y)^{n-} \rightarrow [M(en)_3]_l[(M'_xQ_y)^{n-}]_m$$

The resultant compounds typically have molecular or low dimensional (chain-like) structures, referred to as chalco(genido)metalates [41]. Examples include $[M(en)_3]Hg_2Te_9$, M = Mn [28], Fe [22], $[M(en)_3]In_2Te_6$ [26] and $[Fe(en)_3](enH)SbSe_4$ [35]. Several other metals, such as Ga, La and Mo, have shown similar coordination behaviours in reactions leading to the formation of $[Ga(en)_3]In_3Te_7$ [40], α,β-$[Mo_3(en)_3(Te_2)_3(O)(Te)]In_2Te_6$ [26] and $[La(en)_4Cl]In_2Te_4$ [34].

Those metal ions (e.g. Group 11–12 and Group 13–15 elements) that are chalcophilic and that have less or little tendency to form complex cations with the solvent usually bond directly to the chalcogen elements. In addition to the discrete molecular and one-dimensional chain structures discussed above, the resultant structures are often extended networks of two- or three-dimensions. In most cases, alkali-metal cations incorporate into the structures as counterions. Among numerous examples are $AHgSbQ_3$ (A = Rb, Cs, Q = Se [37b] and A = Rb, Q = Te [29]), $Rb_2Hg_6Se_7$ [38]; Cs_2PdSe_8 [37a], $RbCu_{1.2}Ag_{3.8}Se_3$ and $Cs_2Cu_2Sb_2Se_5$ [37b]. In a few cases, these infinite 2D and 3D networks are intercalated by free solvent molecules (e.g. $Cu_2SbSe_3 \cdot x$en ($x = 0.5, 1$) [36]) or by metal complex cations (e.g. $[Mn(en)_3]Ag_6Sn_2Te_8$ [39] and $[Ga(en)_3]In_3Te_7$ [40]).

A close look at these compounds reveals that most of them are Zintl phases [41] with precise electron count and thus likely to be semicondutors. Physical measurements have been made on many of these compounds to study their optical and

electronic properties. The focus here, however, is on their very rich structural chemistry which will be the subject of the following sections.

3. Chalcogenidometalates

These are molecular species of general formula $[M_xQ_y]^{z-}$ (M = metal, Q = S, Se, Te) [42]. They are sometimes referred to as chalcometalates. Compounds that contain one-dimensional M_xQ_y anionic chains and complex cations are included in this group, but solid state chalcogenides or polychalcogenides with extended two- and three-dimensional framework structures are excluded.

3.1. Group 11–12 compounds

*3.1.1. $[M(en)_3]Hg_2Te_9$, M = Fe (**1**), Mn (**2**)*

$[Fe(en)_3]Hg_2Te_9$ (**1**) is the first tellurometalate obtained by solvothermal reactions in ethylenediamine. Prior to the synthesis of this compound, a number of mercury containing tellurometalates were prepared via other routes, including $(HgTe_2)^{2-}$ [43], $(Hg_2Te_5)^{2-}$ [44], $Hg_4Te_2(Te_2)_2(Te_3)_2]^{4-}$ [44], $(Hg_2Te_4)^{2-}$ [45] and $[Hg_3Te_7(en)_{0.5}]^{4-}$ [45] by solvent extraction of intermetallic alloys and $[Hg(Te_4)_2]^{2-}$ [46,47], $(HgTe_7)^{3-}$ [48,49], and $(Hg_4Te_{12})^{4-}$ [50] by nonaqueous solution phase reactions.

$[Fe(en)_3]Hg_2Te_9$ (**1**) represents a new type of one-dimensional chain structure and the crystal structure of $[Mn(en)_3]Hg_2Te_9$ (**2**) is closely related to **1**. Both crystallize in monoclinic crystal system, space group $P2_1/c$ (no. 14). Both consist of weakly bound Zintl anions $(Hg_2Te_9)^{4-}$ (Fig. 2), formally written as $[(Hg^{2+})_2(Te^{2-})(Te_2^{2-})(Te_3^{2-})_2]$, and metal (Mn, Fe) tris–ethylenediamine cations that are located between the anionic chains. The anion contains a five-membered Hg_2Te_3 ring attached to two $(Te_3)^{2-}$ units through the two Hg in the 1 and 3 positions of the ring. The mercury atoms have trigonal planar coordination. The Hg–Te distances (2.690(2)–2.769(1) Å in **1** and 2.693(2)–2.767(2) Å in **2**) and Te–Te distances (2.733(2)–2.777(2) Å in **1** and 2.733(2)–2.772(2) Å in **2**) are comparable with those reported for $(Hg_4Te_{12})^{4-}$ [50], $Hg_2Te_5^{2-}$ [44], $[Hg_3Te_7(en)_{0.5}]^{4-}$ [45] and $Hg_2Te_4^{2-}$ [45] whose structures are also based on five-membered Hg_2Te_3 rings. The $Hg_2Te_9^{4-}$ anions are connected by weak intermolecular interactions between the two Te_3 from the adjacent anions, at a distance of 3.488(2) Å in **1** (Te(4)–Te(7)) and 3.384(14)Å, 3.523(3)Å in **2** (Te(1B)–Te(4), Te(7)–Te(7)) respectively. This is considerably shorter than the van der Waals distance of 4.12 Å [51] indicating a secondary bonding interaction [52]. The cation, $[M(en)_3]^{2+}$, is present with two independent molecules in the stable conformation lel_3 [53]. Given the centrosymmetric space group of the structure, both enantiomers $\Lambda(\delta\delta\delta)$ and $\Delta(\lambda\lambda\lambda)$ are present [54]. The only difference between **1** and **2** is that all $(Te_3)^{2-}$ pairs are in '*cis*' position in **1** while one third of them are in the '*trans*' position in **2**. The crystal structures of both Fe-trisethylenediamine and Mn-trisethylenediamine have never been reported prior to our study.

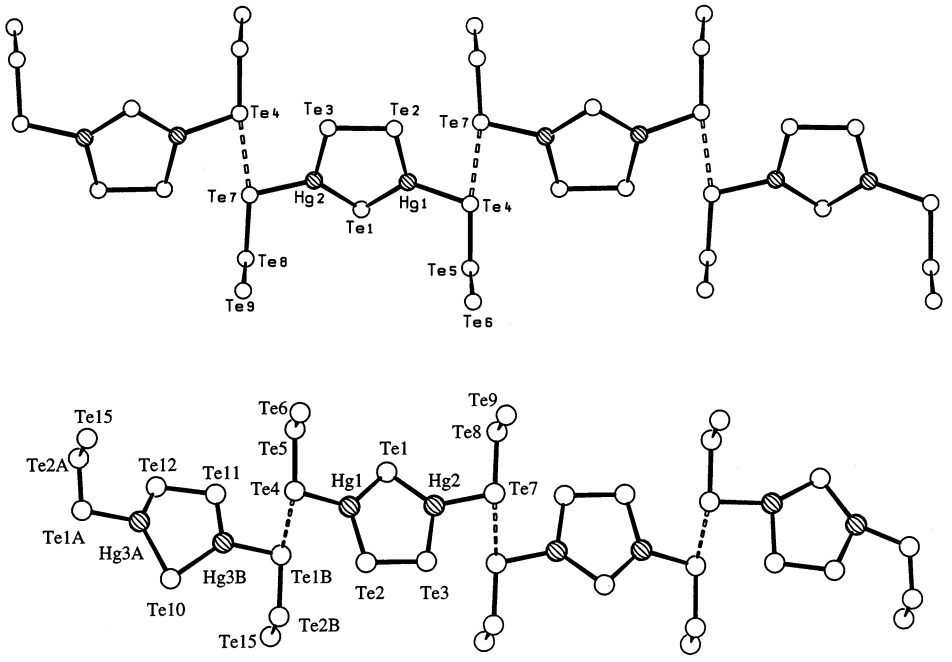

Fig. 2. The $^{1}_{\infty}[Hg_2Te_9^{4-}]$ quasi one-dimensional chain in **1** (top) and **2** (bottom). The weak Te···Te interactions are indicated by dashed lines.

*3.1.2. {[Mn(en)$_3$]$_2$Cl$_2$}Hg$_2$Te$_4$ (**3**)*

The crystal system of **3** is also monoclinic, $P2_1/c$ (no. 14). It contains one-dimensional $^{1}_{\infty}[(Hg_2Te_4)^{2-}]$ anions running along the crystallographic *c*-axis, as shown in Fig. 3. The structure is again built upon the Hg_2Te_3 five-membered rings. These rings are connected through bridging Te(6) to result in a 1D chain. The Hg–Te and Te–Te distances in **3** are similar to those reported for $(Et_4N)_2Hg_2Te_4$ which is isostructural to **3** [45]. The two independent $[Mn(en)_3]^{2+}$ cations exist as different conformers *lel*$_3$ and *lel*$_2$*ob* (or Δ(λλλ) and Δ(λλδ) and theirs enantiomers). The hydrogen bonding between chlorine and some N–H (Cl···N 3.34–3.54 Å) from the

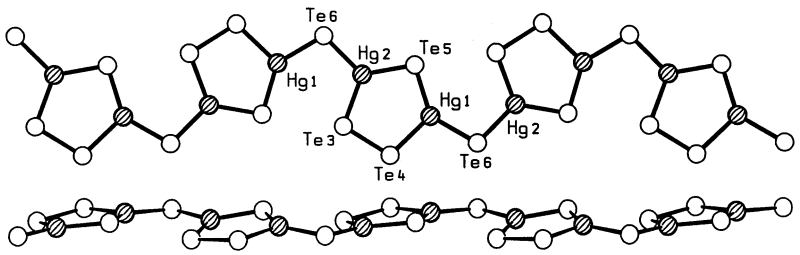

Fig. 3. Two views of the $^{1}_{\infty}[Hg_2Te_4^{2-}]$ one-dimensional chain in **3**.

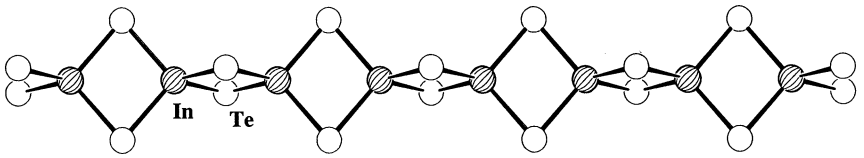

Fig. 4. The $^{1}_{\infty}[In_2Te_4^{2-}]$ one-dimensional chain in **4**.

two independent cations results in a quasi one-dimensional cationic chain, also running along the *c*-axis. The title compound provides the first example of $[M(en)_3]^{n+}$ complex cations that contains two different conformers.

3.2. Group 13–16 compounds

*3.2.1. $[La(en)_4Cl]In_2Te_4$ (**4**)*

Like the mercury compounds described in the previous section, **4** is also a one-dimensional chain compound consisting of metal coordination complex cations and a $(M_xQ_y)^{z-}$ Zintl anions. It crystallizes in a non-centrosymmetric tetragonal space group $I4$ (no. 79). Both the $[La(en)_4Cl]^{2+}$ cations and the $^{1}_{\infty}[(In_2Te_4)^{2-}]$ anions form polymeric chains adjacent to each other and propagate along the *c* axis. The anionic chain may be described as edge-sharing $InTe_4$ (see Fig. 4). Examples of such chain have been observed previously in $AInQ_2$ (A = Na [55], K [55,56], Rb [57], Tl [57] and Q = Te; A = Tl [58] and Q = Se), $A'In_2Te_4$ (A′ = Ca [59], Sr [55], Ba [55]), and in $[(C_4H_9)_4N]_2In_2Te_4$ [60], many of which were prepared by high temperature methods such as direct or chemical vapor transport reactions of elements and/or binary chalcogenides [55,58,59], or by flux growth technique [55]. The In–Te distances [2.779(2), 2.787(2)Å] and angles in **4** are comparable with those reported for these compounds. Only a few indium chalcogenide compounds were prepared via low temperature routes prior to the synthesis of the title compound, including $[(C_4H_9)_4N]_2In_2Te_4$ by electrochemical reactions and $[(C_2H_5)_4N]_5In_3Te_7$ by solution synthesis in liquid ammonia [61].

The $[La(en)_4Cl]^{2+}$ cations pack along the *c*-axis (with nonbonding contact La···Cl of 4.35(1) Å) and have one carbon atom statistically disordered on two positions, resulting in a 50–50% statistic distribution of the two possible chiral conformations ob_4 (δδδδ) and lel_4 (λλλλ). The nona coordination of La describe an undistorted capped square antiprism. To the best of our knowledge this is the only example of [La(bidentate)$_4$(monodentate)] with such a regular coordination. The only other ethylenediamine derivative is $La(en)_4(CH_3CN)(CF_3SO_3)_3$ [62] with a nona coordination describing a tricapped trigonal prism and a predominant conformation of the en ligands of lel_4ob (λλλδ) (and its enantiomer).

*3.2.2. $[M(en)_3]In_2Te_6$, M = Fe(**5**), Zn(**6**)*

Compounds **5** and **6** are isostructural and belong to the non-centrosymmetric orthorhombic crystal system (space group $P2_12_12_1$). The crystal structure contains

linear channels of $[M(en)_3]^{2+}$ cations adjacent to polymeric chains of $^1_\infty[(In_2Te_6)^{2-}]$ anions propagating along the crystallographic *c*-axis. A single anionic chain is shown in Fig. 5(a). The geometry and stereochemistry of the cations are similar to those discussed in the previous sections. The average Fe–N distance in **5** is 2.21(1) Å, in agreement with high spin Fe(II) amine complexes [63] and with those in **1**. The average Zn–N distance, 2.19(2) Å, is also comparable to those reported [64]. The one-dimensional chain of the $(In_2Te_6)^{2-}$ anions is constructed by linking $InTe_4$ tetrahedra via bridging Te and Te_2. It may also be described as alternating fused five-membered rings $[(In^{3+})_2(Te_2^{2-})(Te^{2-})]$, joined at the In atoms. The repeating unit constitutes four In_2Te_3 rings giving a period of 16.27 Å. This results in a 'Vierer' single chain [65]. The In–Te distances [2.761(2)–2.825(1) Å] are comparable with other indium telluride compounds, such as those observed in 1D compounds listed above [55–61] and in **4**. As far as we are aware, $InSe_4$ is the only other indium–chalcogen five-membered ring that has been found in isolated anions $[In_2(Se_4)_2(Se_5)_2]^{4-}$; $[In_2Se_2(Se_4)_2]^{3-}$ and $[In_3Se_3(Se_4)_3]^{3-}$ [66].

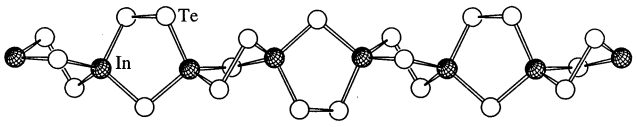

(a) $^1_\infty[In_2Te_6^{2-}]$ in **5,6** period = 16.27 Å

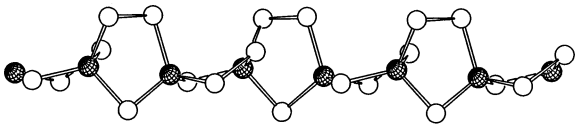

(b) $^1_\infty[In_2Te_6^{2-}]$ in **7** period = 14.50 Å

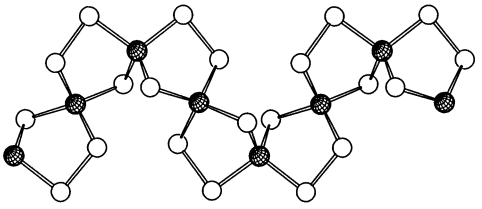

(c) $^1_\infty[In_2Te_6^{2-}]$ in **8** period =11.55 Å

Fig. 5. The $^1_\infty[In_2Te_6^{2-}]$ one-dimensional chain in (a) **5** and **6** with a period of 16.27 Å; (b) **7** with a period of 14.50 Å; and (c) **8** with a period of 11.55 Å.

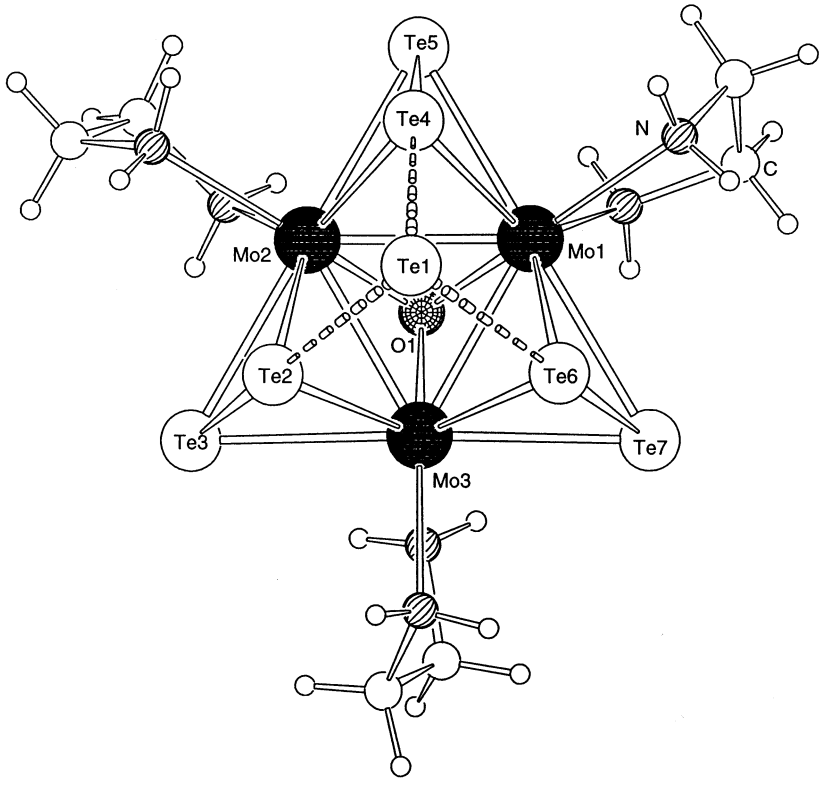

Fig. 6. The $[Mo_3(en)_3(Te_2)_3(O)(Te)]^{2+}$ cation in **7** and **8**.

*3.2.3. α,β-[$Mo_3(en)_3(Te_2)_3(O)(Te)$]$In_2Te_6$ (**7**, **8**)*

The two polymorphs, phase α (**7**) and β (**8**), were isolated from crystal growth of $[Mo_3(en)_3(\mu_2\text{-}Te_2)_3(\mu_3\text{-}Te)(\mu_3\text{-}O)]In_2Te_6$. Both structures are monoclinic ($P2_1/c$, no. 14) and have the same structure motifs in their anionic chains as in **5** and **6**, that is, they also contain one-dimensional chains of fused In_2Te_3 five-membered rings. The major difference lies in the puckering and disposition of these rings along the $^1_\infty[(In_2Te_6)^{2-}]$ chain. The period of the chains are 14.50 Å for **7** and 11.55 Å for **8**, respectively, which are the same as the length of *b*- (**7**) and *c*-axis (**8**), as illustrated in Figs. 5(b and c). The high degree of flexibility of these chains is reflected in the drastic differences in the length of the repeating units among them (16.27 Å in **5** and 16.28 Å in **6**). Since the In–Te and Te–Te bond distances are similar in all four compounds, the very small variations in them do not account for the degree of stretching of the repeated units. The differences in the stretching may be accounted for by considering the In···In long contacts. The stretching factor *f* [67] of each 'Vierer' chain can be calculated as the ratio between the observed period and the sum of the four In···In distances within a period. The results correlates well with the observed period.

Fig. 6 shows the molecular structure of the $[Mo_3(en)_3(\mu_2\text{-}Te_2)_3(\mu_3\text{-}Te)(\mu_3\text{-}O)]^{2+}$ cations which has nearly a C_{3v} symmetry. While the $Mo_3L_3(\mu_2\text{-}Q_2)_3(\mu_3\text{-}Q')$ core has been observed in several other structures with 9-coordinate Mo(IV) atoms [68], where L = terminal ligand (e.g. disulfide S_2^{2-} and diselenide Se_2^{2-}), Q = doubly bridging disulfide or diselenide and Q′ = triply bridging S, Se or O atom, the metal cluster Mo_3 in **7** and **8** represents the first example for Q = Te and Q′ = O. The only other Mo/Te cluster previously reported is $[Mo_3(CN)_6(\mu_2\text{-}Te_2)_3(\mu_3\text{-}Te)]^{2-}$ (Q, Q′ = Te) [69]. The $Mo_3(\mu_2\text{-}Q_2)_3$ part of the core can be described as a triangular Mo_3 with three edge-bridging ditelluride ligands, or as a triplet of Mo corner-sharing Mo_2Te_2 tetrahedra. The bridging Te_2 dimers are elongated (2.82(4) and 2.80(2) Å for **7** and **8**, respectively) compared to the typical covalent bond observed in the chains (av. Te–Te 2.755(8)Å). The tetrahedral units in **7** and **8** have a Mo–Mo bond (2.719–2.733 Å) and a geometry consistent with their sulfide and selenide structures and with the three known examples of $MoMTe_2$ tetrahedra (M = Fe, Te) [70]. In both cases, the addition of a capping O atom at one face (1.29Å from the Mo_3 plane) tilts the Te_2 towards the opposite face to the extent that one Te atom is approximately in the Mo_3 face (see Te3, Te5 and Te7 in Fig. 6). The same motif is found in $[Mo_3(\mu_2\text{-}Q_2)_3(\mu_3\text{-}Q')]^{4+}$ (Q = S, Se) species in which Q′ is an O, S or Se atom at the Mo_3 face capping position and in $[Mo_3(CN)_6(\mu_2\text{-}Te_2)_3(\mu_3\text{-}Te)]^{2-}$. This arrangement allows the three apical Te atoms (Te2, Te4 and Te6 in Fig. 6) to bond to a seventh Te atom, resulting in a Te_3 face capping Te atom (Te1) that is approximately 2.26 Å from the Te_3 plane. This gives rise to a three-tiered pyramid shape for the cation core, and a cubic unit for Mo_3Te_3TeO (see the three Mo and O atoms and Te1, Te2, Te4, and Te6 in Fig. 6). The three terminal ethylenediamine ligands complete the valences of the Mo atoms. The bonding interactions between Te1 at the capping position (Te_{ca}) and the three apical Te atoms (Te_{ap}) are rather strong (3.03(4) Å (av.) for the α-phase and 3.06(6) Å (av.) for the β-phase). These are certainly longer than a typical Te–Te covalent bond distance (2.72–2.75 Å), but considerably shorter than a van der Waals distance (4.12 Å). In other triangular $[Mo(IV)]_3$ compounds with bridging diselenides, similar but weaker intermolecular bonding interactions have been observed between the three apical Se_{ap} and the face capping Se_{ca} (usually from a neighboring cluster unit). It has been observed that molybdenum polyselenide compoud = nds that contain $[Mo_3Se_7]^{4+}$ cluster core generally have a tendency to bind a negatively charged Se_{ca} via Se_{ap} atoms. A rational has been given to account for the striking inverse correlation between the Se_{ca}–Se_{ap} and doubly-bridging Se–Se bond distances [68].

*3.2.4. $[M(en)_3]Sn_2Q_6$, M = Mn, Zn, Q = Se (**9**, **10**), Te (**11**, **12**)*

All four structures are similar. $[M(en)_3]Sn_2Se_6$, M = Mn (**9**), Zn (**10**) and $[Mn(en)_3]Sn_2Te_6$ (**11**) are isostrutural and crystallize in orthorhombic space group *Pbca* (no. 61), while $[Zn(en)_3]Sn_2Te_6$ (**12**) belongs to the monoclinic space group $P2_1/n$ (no. 14). All four are composed of discrete Zintl anions $(Sn_2Se_6)^{4-}$ and metal complex cations $[M(en)_3]^{2+}$ (M = Mn, Zn). The anion is a dimer of edge-sharing tetrahedra of SnQ_4 (Q = Se, Te) and is shown in Fig. 7. The Sn–Q bonds are comparable with those of other Sn/Q compounds, ranging 2.46–2.50 Å (terminal)

and 2.57–2.61 Å (bridging) for Sn–Se, and 2.68–2.75 Å (terminal), 2.79–2.82 Å (bridging) for Sn–Te bonds [71–73]. No direct bonds are formed between the tin atoms in the dimer.

The conformation of the cations is lel_3 for $[Mn(en)_3]^{2+}$ in **9** and **11**, and for $[Zn(en)_3]^{2+}$ in **10**. The enantiomeric isomers are in the Δ(λλλ) and Λ(δδδ) forms, respectively, although with a different ratio in a given asymmetric unit. These compounds are mesomeric since the space group (*Pbca*) is a centrosymmetic one. The conformation of $[Zn(en)_3]^{2+}$ in **12** is lel_2ob-Δ(λλδ). It is, therefore, clear that the difference in the crystal packing (hence the space groups) of the two structure groups is due to the different conformation of the cations (see Fig. 7, bottom). The M–N distances are within the range (2.12–2.40 Å) as observed in **2**, **3** and **6**. The lel_2ob conformer for the Zn complex in **12** has been observed in two compounds reported in the Cambridge Structural Data system, among all nine $[Zn(en)_3]^{2+}$ complexes (two lel_2ob, six lel_3 and one ob_3).

3.2.5. $[Fe(en)_3](enH)SbSe_4$ (**13**)

Single crystal structure analysis reveals that **13** crystallizes in the triclinic system, space group $P\bar{1}$ (no. 2). Its structure contains discrete molecular species: $(SbSe_4)^{3-}$ anions, $[Fe(en)_3]^{2+}$ and $(enH)^+$ cations. Its unit cell is shown in Fig. 8(a). The Sb–Se bond distances range from 2.468(1) to 2.482(1) Å, comparable with those found in related compounds containing $(SbSe_4)^{3-}$ anions, 2.438–2.50 Å [74,75]. Formal oxidation state assignment suggests a Sb(V), Se(–II) and Fe(II). The

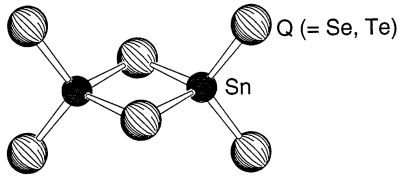

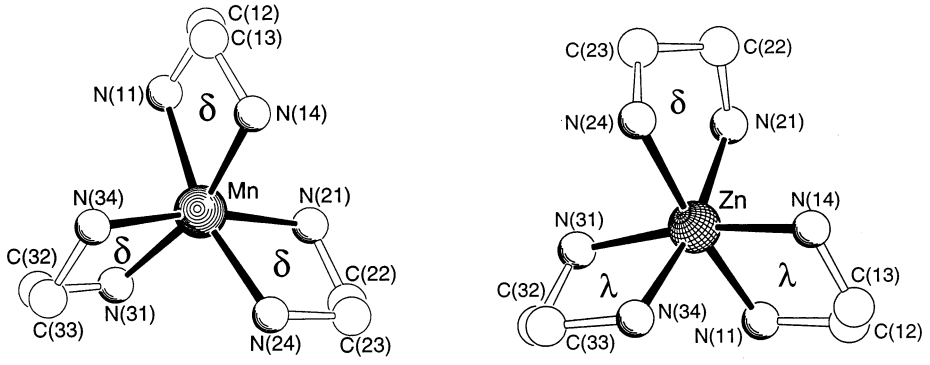

Fig. 7. The Zintl anion $Sn_2Q_6^{4-}$ (Q = Se, Te) in **9**–**12** (top), $[Mn(en)_3]^{2+}$ in **9**, **11** and $[Zn(en)_3]^{2+}$ in **12** (bottom). The different conformations are indicated in the drawings.

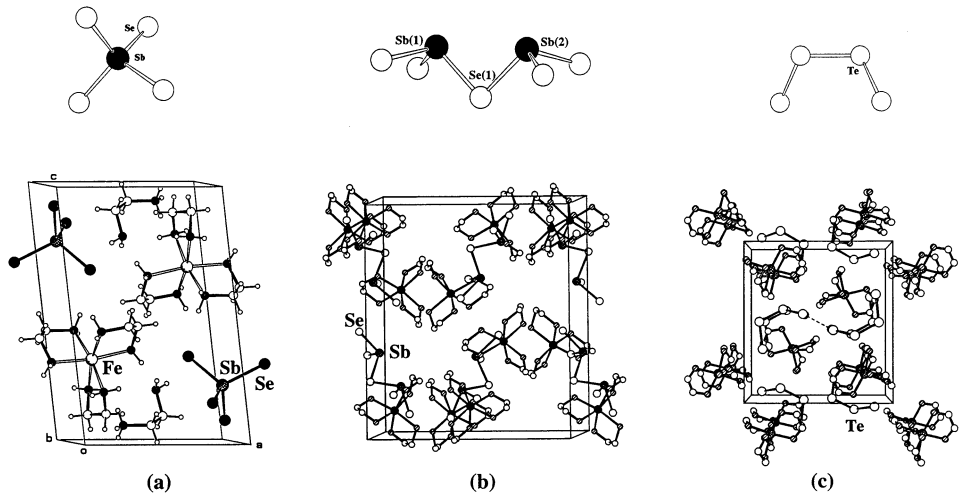

Fig. 8. Views showing unit cells of **13** (a), **14** (b) and **15** (c). The Zintl anions are discrete $SbSe_4^{3-}$ (a), $Sb_2Se_5^{4-}$ (b) and Te_4^{2-} (c) as depicted in the figure.

monoprotonated ethylenediamine cations have been reported previously in several papers [74,76,77]. The average Fe–N distance of 2.21 Å again agrees well with high spin Fe(II) amine complexes and is very similar to those in **1** and **5**. The cation $[Fe(en)_3]^{2+}$ is present in two conformers, 72% as *lel*$_2$*ob* and 28% as *lel*$_3$. Compared to the preparation and crystal analysis of $[Ge(en)_3][enH]SbSe_4$ [74], single crystals of **13** were grown by a relatively easier and simpler route and the solvothermal reactions also produced crystals of suitable size and good quality whose structure determination was carried out at room temperature.

*3.2.6. $[Fe(en)_3]_2Sb_2Se_5$ (**14**)*

The crystal system of **14** is non-centrosymmetric orthorhombic, space group $Pca2_1$ (no. 29), $a = 15.843(3)$ Å, $b = 18.320(4)$ Å, $c = 11.824(2)$ Å, $V = 3432(1)$ Å^3, $Z = 4$. It contains $[Fe(en)_3]^{2+}$ complex cations and discrete $Sb_2Se_5^{4-}$ Zintl anions. Each Sb atom in $Sb_2Se_5^{4-}$ is surrounded by three selenium atoms to give a trigonal coordination. Of the five crystallographically independent selenium atoms, Se(1) is a bridging ligand to link Sb(1) and Sb(2), and the other four are terminal ligands as shown in Fig. 8(b). The Sb–Se distances, 2.482(4)–2.606(4) Å, are slightly longer than those in **13**. The conformation of the two $[Fe(en)_3]^{2+}$ cations are both *lel*$_3$-Δ(λλλ). The ethylenediamine (en) functions as a bidentate ligand and forms a five-menbered chelate ring with iron atom, the latter has a distorted octagonal coordination with six nitrogen atoms from en giving an average Fe–N bond distance of 2.22(2) Å, again in agreement with high spin Fe(II) amine complexes [63] and with those in **1**, **5** and **13**.

3.2.7. $[Mn(en)_3]Te_4$ (15)

The synthesis of compound **15** presents another example in which polychalcogen Q_y^{2-} species form under soft solvothermal conditions. The compound belongs to monoclinic space group $P2_1/n$ (no. 14), $a = 8.461(2)$ Å, $b = 15.653(2)$ Å, $c = 14.269(2)$ Å, $\beta = 91.37(1)°$, $V = 1889.3(4)$ Å^3, $Z = 4$. The structure is very simple, consisting of discrete $[Mn(en)_3]^{2+}$ cations and Te_4^{2-} anions (Fig. 8(c)). The Te–Te distances in the Te_4^{2-} unit, 2.709(1)–2.751(1) Å, are comparable to those found in **1** (2.733(2)–2.777(2) Å), **2** (2.733(2)–2.772(2) Å), **3** (2.751(2) Å), **5** (2.753(2)–2.754(2) Å) and **6** (2.575(1)–2.759(1) Å). There is also a fairly short contact between each pair of Te_4^{2-} anions (Te(4)···Te(4) = 3.329(1) Å, indicated by dashed lines in the figure), compared to those of 3.488(2) Å in **1** and 3.384(14) and 3.523(3) Å in **2**. The manganese atom is surrounded by six nitrogen atoms to give a familiar octahedral coordination. The conformation of $[Mn(en)_3]^{2+}$ is *lel*$_2$*ob* with a configuration of Δ(λλδ) and Λ(δδλ) according to Saito's description [54].

4. Intercalated layer structures

These structures contain layers of covalent network and molecular species (metal complex cations or organic molecules) that intercalate between the layers. The interlayer distances are usually large so that the direct interactions between the adjacent layers are negligible.

4.1. $Cu_2SbSe_3 \cdot 0.5en$ (16) and $Cu_2SbSe_3 \cdot en$ (17)

Compounds **16** and **17** represent a novel structure type that incorporates both inorganic and organic components into the structure. Both compounds belong to monoclinic crystal systems (**16**: centrosymmetric $P2_1/c$, no. 14; **17**: non-centrosymmetric *Pn*, no. 7). Both contain two-dimensional Cu_2SbSe_3 layers with free ethylenediamine molecules sandwiched between these layers. Within each layer, the antimony atom Sb(1) bonds to Cu(1), Se(1), Se(2) and Se(3) to result in a tetrahedral coordination (see Fig. 9). The average Sb–Se distance, 2.572 Å for both structures, is comparable with those of the three known copper selenoantimonate compounds, $CuSbSe_2$ [78], Cu_3SbSe_3 [79] and Cu_3SbSe_4 [80]. The Sb(1)–Cu(1) bond lengths, 2.672 Å in **16** and 2.656 Å in **17**, are considerably shorter than those found in the known phases. The Sb(1)–Cu(2) distance is 3.168(2) and 3.239(2) Å in **16** and **17**, respectively, similar to that found in Cu_3SbSe_3 (3.165(3) Å). Cu(1) to Se coordination is trigonal while Cu(2) to Se is nearly trigonal planar. The average Cu(1)–Se and Cu(2)–Se distances are 2.445(2), 2.394(2) Å in **16** and 2.466(2), 2.409(3) Å in **17**. These are again comparable with those observed in the three known compounds. There is also a short contact between Cu(1) and Cu(2), 2.674(2) Å in **16** and 2.649(3) Å in **17**, compared to the Cu(1)–Cu(2) distances of 2.665 Å in Cu_3SbSe_3 and 2.830 Å in Cu_3SbSe_4. No short Se–Se contacts are found in the two structures. Formal oxidation state assignment suggests a mixed valence for the two coppers, Cu(I) and Cu(II), assuming a $+3$ for Sb and a -2 for Se. This is

consistent with our preliminary results from EPR and magnetic susceptibility measurements, although a more thorough investigation is underway to confirm it. The main difference between the two structures is the orientation of the free ethylenediamine molecules that are situated between the Cu_2SbSe_3 layers. The en molecules are approximately parallel to the Cu_2SbSe_3 layers in compound **16**, and are perpendicular to the Cu_2SbSe_3 layers in compound **17**, as shown in Fig. 9. The inter-layer distances are approximately 5 Å (**16**) and 6.8 Å (**17**), respectively. Both compounds contain copper atoms of mixed-valence, Cu(I) and Cu(II).

4.2. $[Ga(en)_3]In_3Te_7$ (**18**)

The crystal system of **18** is monoclinic ($P2_1/c$, no. 14) with $a = 10.460(2)$ Å, $b = 16.981(3)$ Å, $c = 14.994$ (6) Å, $\beta = 95.46(2)°$, $V = 2651.2(13)$ Å^3, $Z = 4$. The structure of **18** represents a new layered type (Fig. 10). The $In_3Te_7^{3-}$ layers contain three crystallographically independent In atoms, all of which have a tetrahedral coordination with Te atoms. Out of the seven Te atoms, two of which form a dimer, Te_2^{2-}, and a formal oxidation state assignment gives $(In^{3+})_3(Te_2)^{2-}(Te^{2-})_5$. The resultant two-dimensional network is a Zintl anion. The In–Te distances, 2.748(1)–2.826(1) Å, are comparable with those observed in **4–8**. The molecular $[Ga(en)_3]^{3+}$ are intercalated between the anionic layers. The conformation of the two independent cations is lel_2ob with a configuration of $\Delta(\lambda\delta\delta)$ and $\Lambda(\delta\lambda\lambda)$.

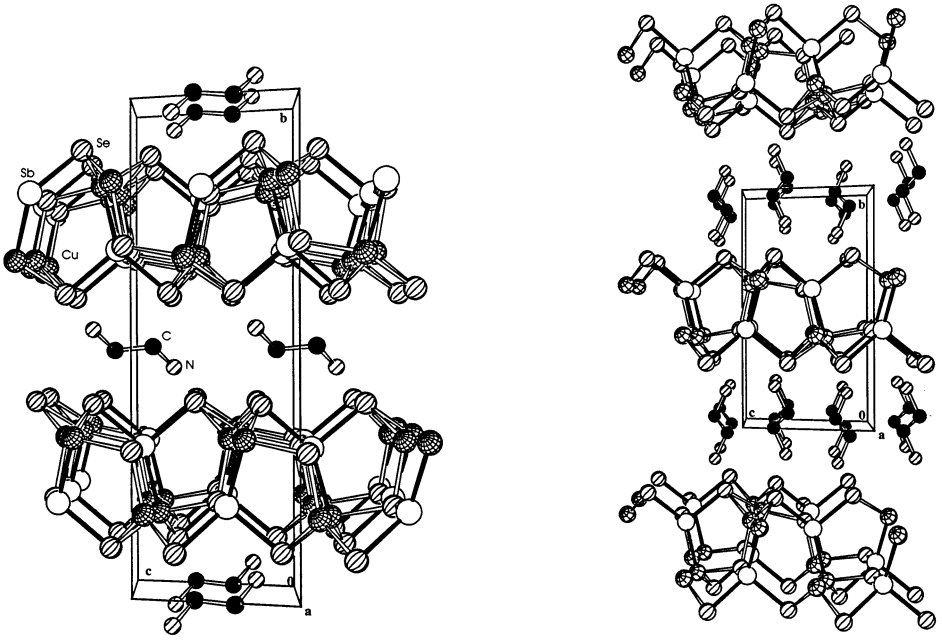

Fig. 9. Perspective views of **16** (left) and **17** (right).

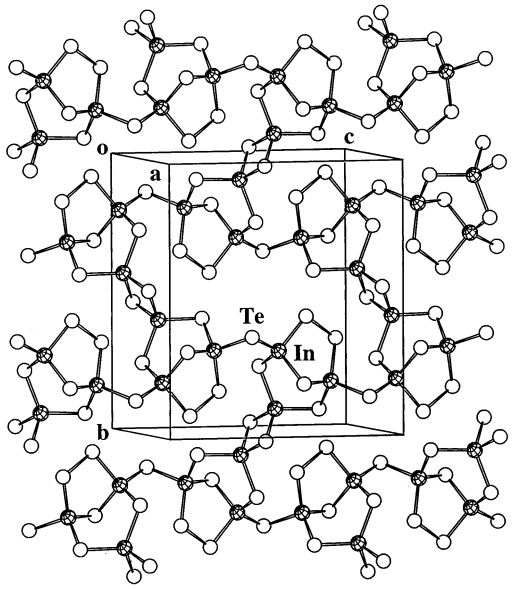

Fig. 10. View showing a single $^{2}_{\infty}[In_3Te_7^{3-}]$ layer along the *a*-axis.

5. Intermetallic framework structures

Compounds in this category do not have metal complex cations nor molecular solvent species incorporated in their structures. In all examples given below, the alkali metals enter the final products as counter ions. The Group 10–12 metals combine with the chalcogens to form extended (2D or 3D) metal chalcogenide networks while the counter ions fill the spaces between the layers or in the voids and open channels.

5.1. Group 10 metal chalcogenide

*5.1.1. Cs_2PdSe_8 (**19**)*

Compound **19** is the first alkali-metal palladium chalcogenide synthesized from ethylenediame medium (tetragonal crystal system, $I4_1/acd$, no. 142). It contains a three-dimensional $^{3}_{\infty}[(PdSe_8)^{2-}]$ open framework based on $[Pd(Se_4)_2]^{2-}$ building blocks. The Pd atoms have a square-planar coordination with four terminal Se atoms from the four $(Se_4)^{2-}$ ligands. The neighboring Pd atoms bridge themselves through $(Se_4)^{2-}$ to give an extended structure, as shown in Fig. 11. The Cs^+ counterions fill in the open spaces around each $Pd(Se)_4$ unit giving Cs···Se(1) distances of 3.575 Å × 2, 3.649 Å × 2, 3.862 Å × 2 and a Cs···Se(2) distance of 3.803 Å × 2. An interesting feature in this structure is the formation of the two 3D $^{3}_{\infty}[Pd(Se_4)_2]^{2-}$ sublattices **A** and **B** (Fig. 11) that are topologically identical and mutually insertional. The Pd atoms in the two sublattices reside at a single

crystallographic site. The sub-framework (**A** or **B**) is built upon connecting the neighboring $[Pd(Se_4)_2]^{2-}$ units which results in a 3D assembly that resembles alternating right- and left-handed helices running along the *c*-axis. The overall structure results upon insertion of the two sublattices in which the Pd(**A**) and Pd(**B**) atoms merge at a distance of 6.453 Å (along the ***c***-axis). The square-planar $Pd(Se_4)$

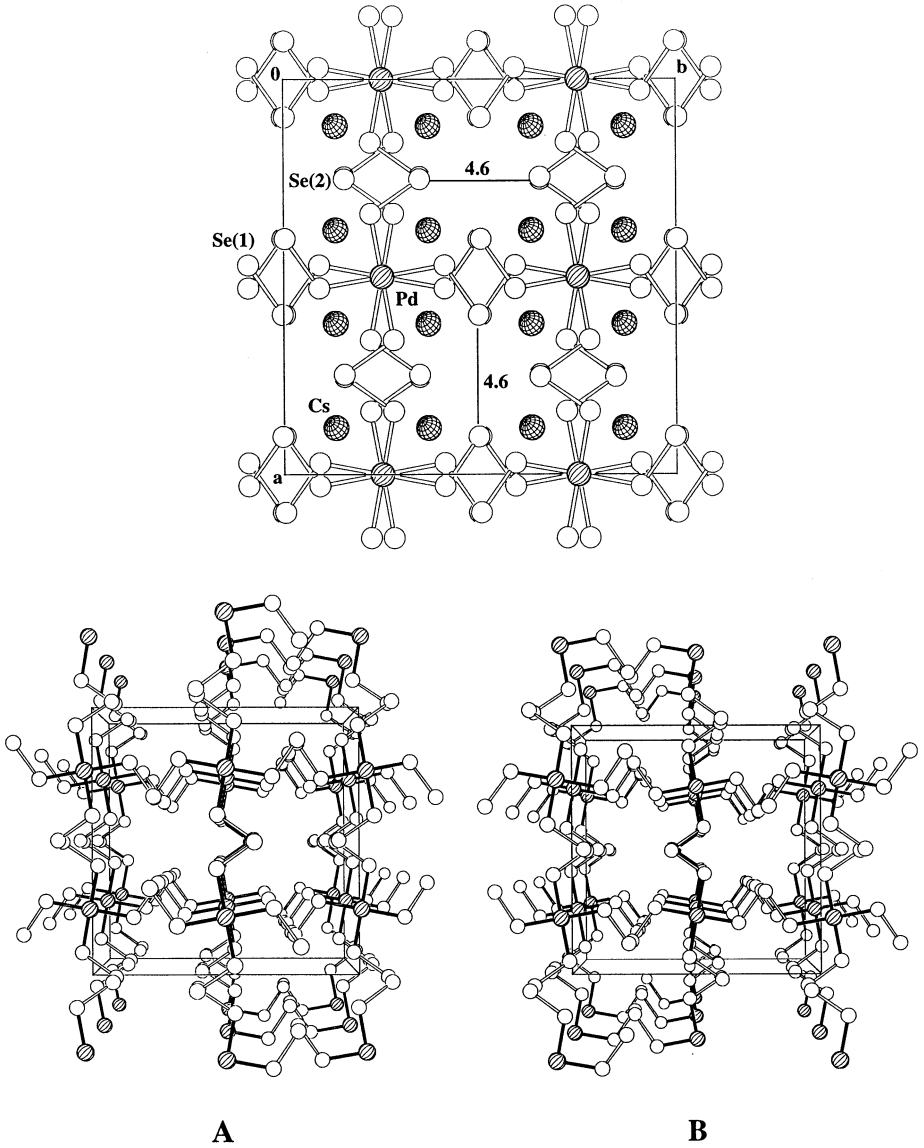

Fig. 11. Crystal structure of **19** projected along the *c*-axis (top) and perspective views showing the two sub-frameworks (bottom).

motifs in the two sub-frameworks give rise to a 'staggered' configuration as shown in Fig. 11.

The K_2PdSe_8 structure is closely related to K_2PdSe_{10} [7d] in that both contain the same $[Pd(Se_4)_2]^{2-}$ unit. However, K_2PdSe_{10} also has a second structural motif, $^3_\infty[Pd(Se_6)_2]^{2-}$, which interpenetrates rather than inserting with the $^3_\infty[Pd(Se_4)_2]^{2-}$ sublattice to generate a 3D network. The Pd–Se bond length in **19** is 2.428(1) Å, slightly shorter than the average Pd–Se distance of 2.465(9) Å in K_2PdSe_{10}. The Se–Se distances in the $(Se_4)^{2-}$ ligands are similar in the two structures, 2.356(2) and 2.34(1) Å, respectively. There are several mutually perpendicular open channels in **19** that run parallel to the three crystallographic axes. The approximate dimensions of these channels are 4.6×4.6 Å along the *c*-axis, and 7.5×3 and 4×3 Å along the *a*- and *b*-axes.

5.1.2. Cs_2PdSe_{16} (**20**)

Compound **20** was synthesized under similar solvothermal conditions as for **19**. It belongs to tetragonal crystal system, non-central symmetric space group $P\bar{4}b2$ (No. 117). The structure of **20** consists of alternate layers of $[CsPd(Se_4)_2]^-$ and $[CsSe_8]^+$. Fig. 12 shows two views along *c* (top) and *a* (bottom) directions, respectively. The palladium atoms reside at Wyckoff position 2*b* and are bonded by four Se_4^{2-} units to form a square-planar coordination. Each Se_4^{2-} functions as a μ_2-ligand through its two terminal Se atoms which connect two neighboring palladium atoms to give rise to a two-dimensional $^2_\infty[Pd(Se_4)_2]^{2-}$ network parallel to the *ab* plane. This network can also be described as composed of fused 20-membered rings $[(PdSe_4)_4]$ with a ring size of about 7×7 Å^2. A cesium cation (Cs1) is accommodated at the center of each ring. In the $Cs(Se_8)$ layer, the Se_8 forms a neutral 8-membered ring with a crown-like shape and with its center located at Wyckoff positions 2*c* and the Cs cations (Cs2) occupy the unit cell corners and faced-centered positions (Wyckoff positions 2*a* and 2*d*) between the Se_8 units. While neutral crown-like Te_8 motif has been observed in Cs_3Te_{22} and Cs_4Te_{28} alkali-metal polytelluride compounds [9], no selenium analogues have been reported prior to the synthesis of **20**. The unique Pd–Se1 interatomic distance is 2.430(2) Å, almost identical to that in **19**. The Se–Se distances in $(Se_4)^{2-}$ are 2.347(4) and 2.347(5) Å, respectively for Se1–Se2 and Se2–Se2, also very similar to that of **19**, 2.356 Å. Three Se–Se distances are observed in Se_8 with 2.367(6), 2.357(3) and 2.357(1) Å, respectively, for Se3–Se3, Se3–Se4, and Se4–Se4.

5.2. Group 11–12 metal chalcogenides

5.2.1. $RbCu_{1.2}Ag_{3.8}Se_3$ (**21**)

Compound **21** is a quaternary intermetallic phase rich in metal content (metal:chalcogen ratio, 6:3). It crystallizes in tetragonal space group P4/nbm (no. 125). Its two-dimensional structure contains alternating $^2_\infty[(Cu_{1.2}Ag_{3.8}Se_3)^-]$ slabs and Rb^+ counterion layers (Fig. 13). Certain structural relations may be drawn between **21** and $CsFe_{0.72}Ag_{1.28}Te_2$ [81] and $KCuZnTe_2$ [82], both belong to the $ThCr_2Si_2$ type [83]. There are two independent metal positions within a single layer

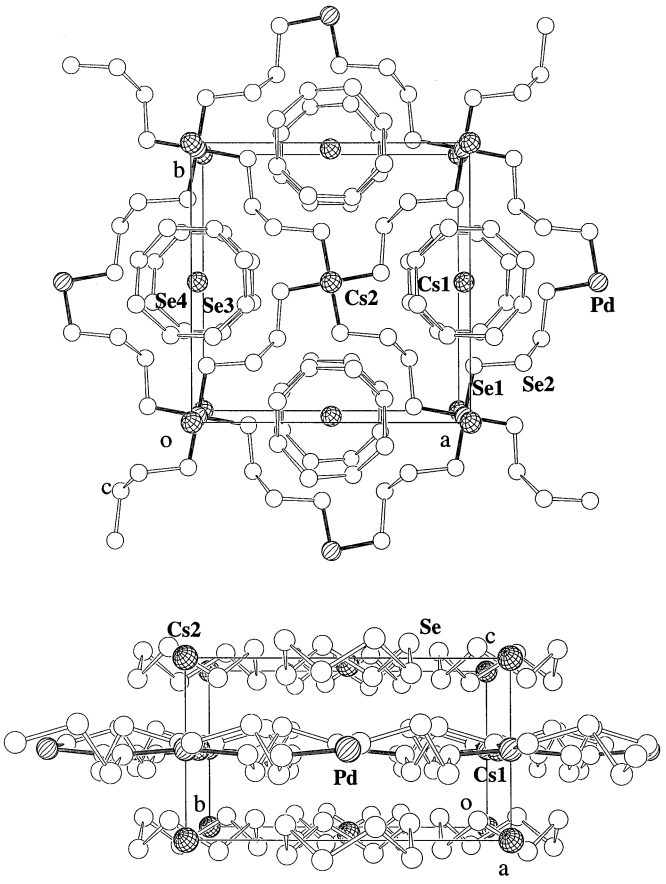

Fig. 12. Two views of **20**. Top: projection along the *c* axis. Bottom: projection along the *a* axs.

of **21**. Position 2a is occupied by Ag and position 8m are shared randomly by both Ag and Cu, labeled as M. Ag(1) has a square planar coordination with Se(1). The Ag(1)–Se(1) distance, 2.996(1) Å, is significantly longer than those found in $Rb_2NbAgSe_4$ (2.640 Å) [84] where Ag has a different, tetrahedral coordination to Se atoms, $K_5Ag_2As_3Se_9$ (av. 2.676 Å) [85] and KAg_3Se_2 (av. 2.794 Å) [86] where Ag has a trigonal coordination with Se. The square planar geometry of Ag is rare, and there are no known examples of this geometry reported for the A–Ag–Se systems. The M (Ag/Cu) atoms bond to three Se to give a trigonal coordination [M–Se(1) = 2.666(1) Å and M–Se(2) = 2.571(1) Å × 2]. The M–Se distances compare reasonably well with those in $RbCuSe_4$ (2.703 Å) [87] and in the aforementioned silver compounds. It is worth mentioning that the coordination of Se(1) atoms is very unusual in this compound. They reside in the interior of the layers and are eight-fold coordinated, four to Ag(1) (in the center of the Ag_4 square) and four to M (in the center of the M_4 tetrahedron). While high coordination number is

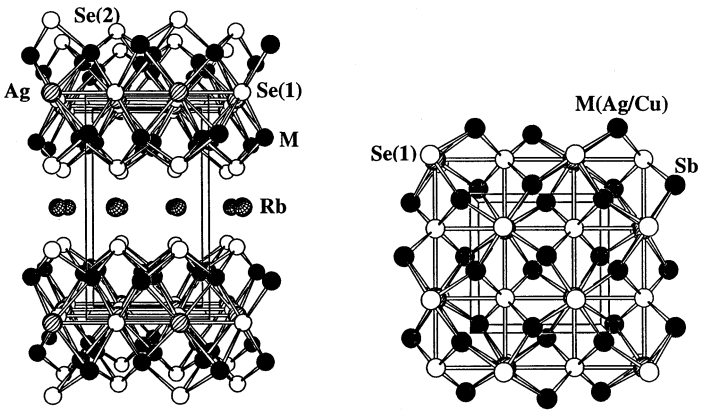

Fig. 13. Left: a perspective view of **21** showing the $^{2}_{\infty}[(Cu_{1.2}Ag_{3.8}Se_3)^-]$ 2D layers and Rb^+ cations located between the layers. Right: a single layer of $^{2}_{\infty}[(Cu_{1.2}Ag_{3.8}Se_3)^-]$.

common for chalcogen elements, encapsulation of these atoms by metals is very unusual. To the best of our knowledge, **21** is the first compound containing 8-coordinated chalcogens that are encapsulated by the metal elements.

*5.2.2. $Cs_2Cu_2Sb_2Se_5$ (**22**)*

Compound **22** is also a quaternary intermetallic chalcogenide with a new type of layered structure (triclinic, space group $P\bar{1}$, no. 2). A perspective view of its crystal structure along the *b* axis is given in Fig. 14. It contains $^{2}_{\infty}[(Cu_2Sb_2Se_5)^{2-}]$ layers stacking along the *b* axis and Cs^+ double layers between the anionic layers. The Sb atoms have a trigonal geometry and the Cu atoms are tetrahedrally coordinated. The two μ_4-bridging Se atoms each bonds to three Cu and a Sb, while the three μ_2-bridging Se atoms each bonds to two metals (M = Cu, Sb). The anionic layer can be constructed by connecting the edge-sharing $CuSe_4$ tetrahedral chains with bridging Sb_2Se_3 units, or can be regarded as composed of fused 12-membered,

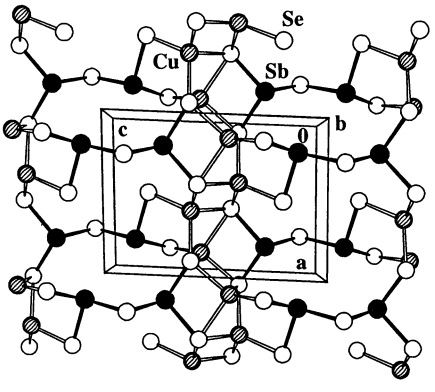

Fig. 14. A view of the $^{2}_{\infty}[(Cu_2Sb_2Se_5)^{2-}]$ two-dimensional layer in **22**.

alternating M–Se rings linked by inter-ring Cu–Se and Sb–Se bonds. The approximate dimension of these rings is 4.6 × 7.0 Å. The Cu–Se bond distances range from 2.410 to 2.596 Å, slightly shorter than that found in **21** (2.571, 2.666 Å) and in $RbCuSe_4$ (2.703 Å) [87]. The Sb–Se distances range 2.515–2.625 Å, compared well to those in **13–14**, **16–17**. Relatively short metal–metal contacts are found between the copper atoms, 2.748 Å for Cu(1)–Cu(1) and 2.678 Å for Cu(1)–Cu(2). These are similar to 2.674 Å in **16**, 2.649 Å in **17**, 2.665 Å in Cu_3SbSe_3 [79], and 2.830 Å in Cu_3SbSe_4 [80].

5.2.3. $Rb_2Hg_3Te_4$ (**23**)

The structure of **23** is a unique layered type (orthorhombic, space group *Pbcn*, no. 60). The $^2_\infty[Hg_3Te_4^{2-}]$ two-dimensional networks are seperated by Rb^+ cations. The top portion of Fig. 15 shows these layers and the Rb^+ cations. The interlayer Te–Te distances are longer than the van der Waals distance of 4.12 Å, which eliminates any significant Te–Te interactions. The $^2_\infty[Hg_3Te_4^{2-}]$ layer is formed by interconnecting six- and eight-membered rings of alternating mercury and tellurium atoms, Hg_3Te_3 and Hg_4Te_4, (see Fig. 15, bottom). The Hg_2Te_3 five-membered ring is quite common, as found in **1–3** and in $Hg_2Te_5^{2-}$ [44], $Hg_3Te_7^{4-}$ [45], but rare for six- and eight-membered mercury–tellurium rings observed in **23**. We believe such a structure motif has not been reported previously. There are two independent Hg sites. Hg(2) has a distorted tetrahedron with four long Hg–Te bonds (2.845(1) Å × 2, 2.848(1) Å × 2), while coordination of Hg(1) is a less common planar one (close to a T-shape), with two short and one long bond (2.693(1), 2.710(1) and 2.905(1) Å). These distances are comparable with those found in **1–3**, and in $Hg_2Te_5^{2-}$, $Hg_4Te_{12}^{4-}$ [44], $Hg_3Te_7^{4-}$ [45], and $Hg(Te_4)_2$ [46,47].

5.2.4. $AHgSbSe_3$ (A = Rb (**24**), Cs (**25**)) and $RbHgSbTe_3$ (**26**)

All three compounds were synthesized in en solution at 170–180°C. Their crystal structures are closely related. Compound **24** crystallizes in monoclinic system, space group $P2_1/c$ (no. 14). Compounds **25** and **26** are isostructural and belong to the orthorhombic space group *Cmcm* (no. 63).

Compounds **24–25** represent a new layered structure. As shown in Fig. 16 (top), the structure consists of $^2_\infty(HgSbQ_3^-)$ (Q = Se, Te) two dimensional network and A^+ (A = Rb, Cs) cations that are placed between the layers. Each layer may be constructed by linking rows of corner-sharing HgQ_4 tetrahedra running parallel to the *c*-axis through the trigonally coordinated SbQ_3 via its bridging Q atoms. The Hg–Q bonds are Hg–Se(1) = 2.748(3) Å × 2, Hg–Se(2) = 2.595 (3) Å × 2 in **25**; Hg–Te(1) = 2.790(2) Å × 2, Hg–Te(2) = 2.901(2) Å × 2 in **26**. The Sb atoms are disordered in both structures having three short and three long contacts with Se (**25**: 2.851(4) Å, 2.780(3) Å × 2, 3.120(4) Å, 3.347(3) Å × 2) and Te (**26**: 2.925(4) Å, 2.906(3) Å × 2, 3.341(4) Å, 3.514(3) Å × 2). The interlayer Q(2)···Q(2) interactions are characteristic of a van der Waals' type.

The structure of **24** is very similar to that of **25** and **26**. The only difference is that the disorder of the antimony in **25–26** is not observed in this structure (Fig. 16, bottom). There are three crystallographically independent Se atoms in **24** (two in **25** and **26**). The Hg–Se distances, 2.608(2)–2.759(2) Å, and Sb–Se distances,

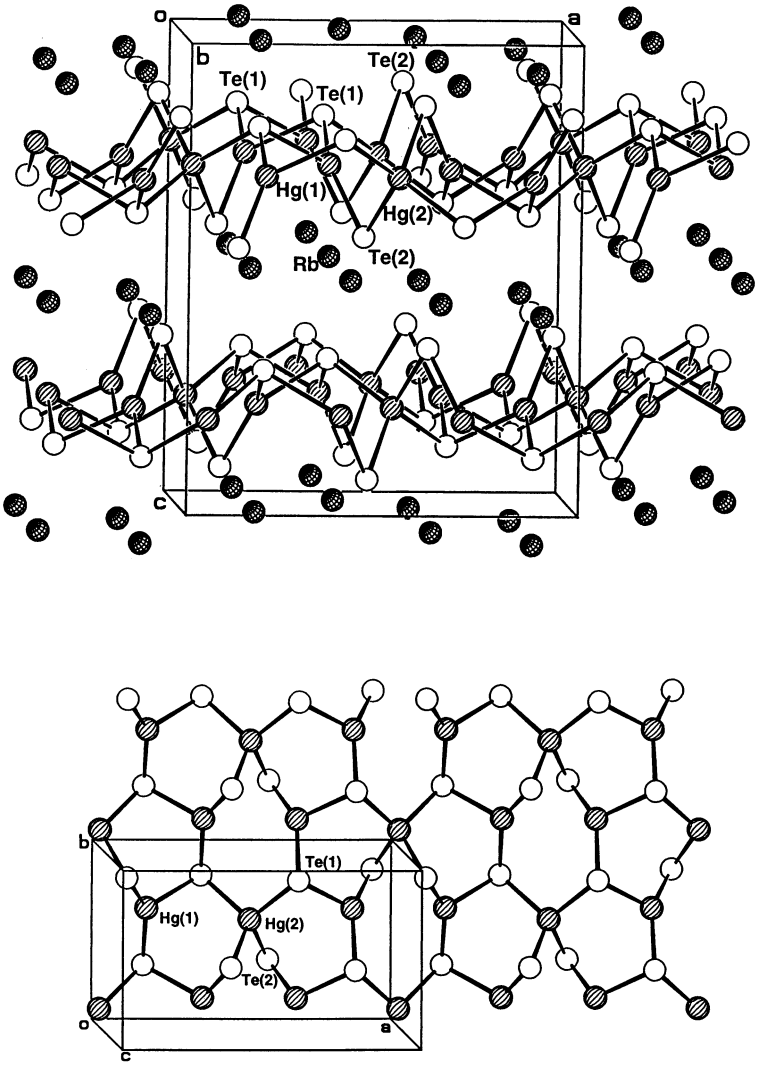

Fig. 15. Crystal structure of **23** showing a perspective view along the *b* axis (top) and a single layer of $^{2}_{\infty}[(Hg_3Te_4)^{2-}]$ (bottom).

2.591(3)–2.615(2) Å, are typical for an average Hg–Se and Sb–Se bond, and comparable with those discussed in the previous sections.

6. Summary

In this article, we have discussed recent development in the synthesis and crystal growth of metal chalcogenides via soft solvothermal reactions ($< 200°C$) in

ethylenediamine medium. The work presented clearly shows that the synthetic route is suitable and promising for this class of compounds, many exhibit interesting structures and unique properties but are metastable or low-temperature phases that either can not be synthesized or are not stable at high temperatures. While high temperature synthesis often produce monochalcogenide phases, retention of polychalcogen units is possible only under mild, low temperature conditions and is the first step towards molecular-building block approach for construction of solid state structures with specific shapes and specified functions and properties.

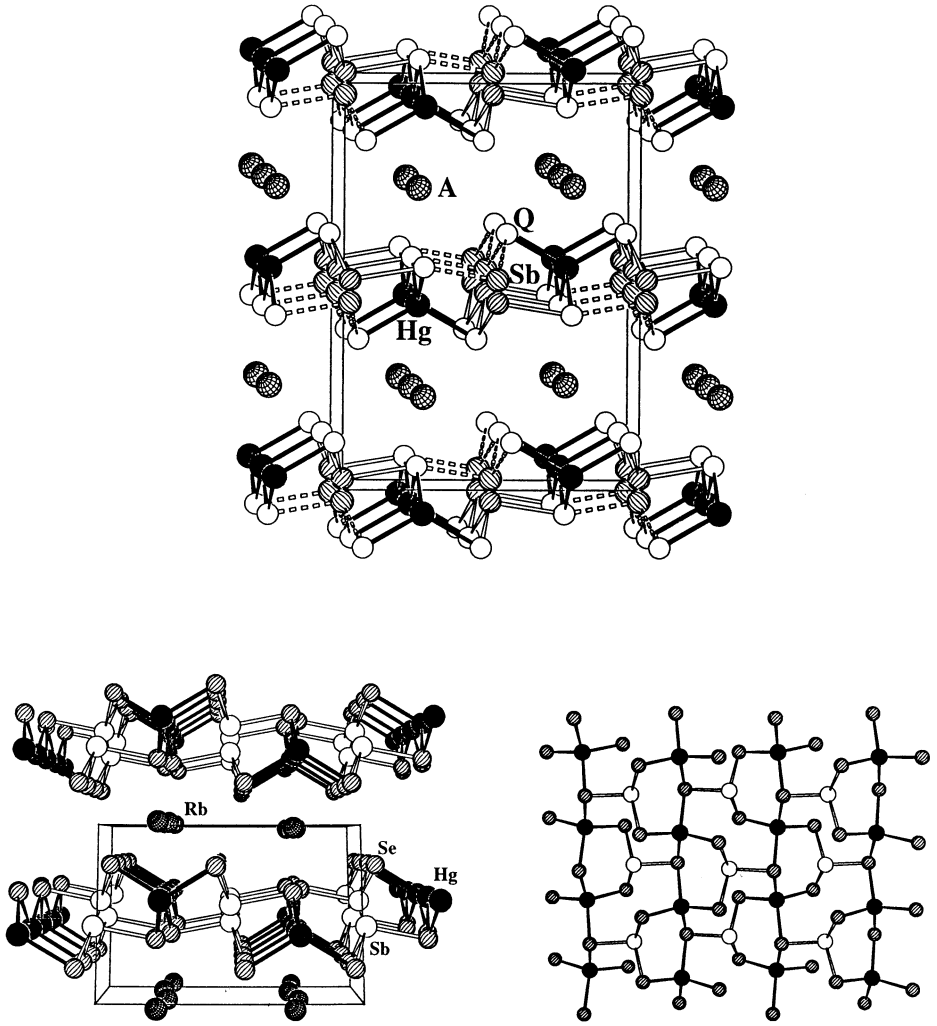

Fig. 16. Crystal structures of **24**–**26**. Top: view along the *a* axis showing disordered Sb atoms (bonds of one set indicated by dotted lines). Bottom: view along the *c* axis (left) and a single layer of $^{2}_{\infty}[(HgSbSe_3)^-]$.

Acknowledgements

Financial support from the National Science Foundation (Grant DMR-9553066 and supplement funds) is greatly appreciated. J.L. would like to thank Camille and Henry Dreyfus Foundation for the Henry-Dreyfus Teacher-Scholar Award. We also thank Professors H.-Y. Guo and P. Wang for their contributions to the solubility measurements, and X.-Y. Huang for his help in plotting some of the figures.

References

[1] (a) R.A. Laudise, in: Progress in Inorganic Chemistry, vol. III, Interscience, New York, 1962. (b) R.M. Barrer, Hydrothermal Chemistry of Zeolites, Academic Press, London, 1982. (c) A. Rabenau, Angew. Chem. Int. Ed. Engl. 24 (1985) 1026. (d) R.A. Laudise, C&EN News, 30 (1987) September 28.

[2] See for example:. (a) Ref. [1]. (b) D.W. Breck, Zeolite Molecular Sieves, Structure, Chemistry and Use, Wiley, New York, 1974. (c) J.D. Corbett, Chem. Rev. 85 (1985) 383. (d) K.H. Lii, R.C. Haushalter, J. Solid State Chem. 69 (1987) 320. (e) R.C. Haushalter, F.W. Lai, ibid. 76 (1988) 218. (f) R.C. Haushalter, F.W. Lai, Science, 246 (1989) 1289. (g) L.A. Mundi, K.G. Strohmaier, D.P. Goshorn, R.C. Haushalter, J. Am. Chem. Soc. 112 (1990) 8182. (h) R.C. Haushalter, L.A. Mundi, Inorg. Chem. 29 (1990) 157. (i) R.C. Haushalter, L.A. Mundi, Chem. Mater. 4 (1992) 31. (j) L.M. Meyer, R.C. Haushater, ibid. 6 (1994) 349.

[3] See for example: (a) M.S. Whittingham, A.J. Jacobson, Intercalation Chemistry, Academic Press, New York, 1982. (b) J. Rouxel, R. Brec, Ann. Rev. Mater. Sci. 16 (1986) 137. (c) R.L. Bedard, S.T. Wilson, L.D. Vail, J.M. Bennett, E.M. Flanigen, in: R.L. Bedard, S.T. Wilson, L.D. Vail, L.M. Bennett, E.M. Flanigen (Eds.), The Next Generations: Synthesis, Characterization and Structure of Metal–Sulfide-based Microporous Solids, vol. 49, Elsevier, Amsterdam, 1989. (d) R.L. Bedard, L.D. Vail, S.T. Wilson, E.M. Flanigen, US Patent 4 880 068, 1989; 4 933 068, 1990. (e) J.B. Parise, Y. Ko, J. Rijssenbeck, D.M. Nellis, K. Tan, S. Koch, J. Chem. Soc. Chem. Commun. (1994) 527. (f) K. Tan, Y. Ko, J.B. Parise, A. Darovsky, Chem. Mater. 8 (1996) 448. (g) G.D. Mahan, J.O. Sofo, Proc. Natl. Acad. Sci. USA 93 (1996) 7436. (h) A.P. Ramirez. Nature, 386 (1997) 156.

[4] (a) A. Stein, S.W. Keller, T.E. Mallouk, Science 259 (1993) 1558. (b) W.S. Sheldrick, M. Wachhold, Angew. Chem. Int. Ed. Engl. 36 (1997) 206.

[5] (a) H.A. Graf, H. Schäfer, Z. Naturforsch. Teil B 27 (1972) 735. (b) H.A. Graf, H. Schäfer, Z. Anorg. Allg. Chem. 414 (1975) 211, 220. (c) K. Volk, H. Schäfer, Z. Naturforsch. Teil B, 33 (1978) 827. (d) G. Dittmar, H. Schäfer, Z. Anorg. Allg. Chem. 441 (1978) 93, 98. (e) K. Volk, K. Schäfer, Z. Naturforsch. Teil B 34 (1979) 172, 1637. (f) B. Eisenmann, H. Schäfer, ibid., 34 (1979) 383. (g) G. Cordier, H. Schäfer, C. Schwidetzky, Rev. Chim. Minér. 22 (1981) 722. (h) G. Cordier, H. Schäfer, C. Schwidetzky, Z. Naturforsch. Teil B 39 (1984) 131.

[6] (a) W.S. Sheldrick, J. Kraub, Z. Naturforsch. Teil B 40 (1985) 571, 1130. (b) W.S. Sheldrick, J. Kraub, ibid. 535 (1986) 179. (c) W.S. Sheldrick, Z. Anorg. Allg. Chem. 562 (1988) 23. (d) W.S. Sheldrick, B. Schaaf, Z. Anorg. Allg. Chem. 620 (1994) 1041. (e) J.B. Parise, J. Chem. Soc. Chem. Commun. (1990) 1553.

[7] (a) Liao, J.-H.; Kanatzidis, M. G. J. Am. Chem. Soc., 1990, 112, 7400. (b) J.-H. Liao, M.G. Kanatzidis, Inorg. Chem. 31 (1992) 431. (c) J.-H. Liao J. Li, M.G. Kanatzidis, ibid. 34 (1995) 2658. (d) K.-W.Kim, M.G. Kanatzidis, J. Am. Chem. Soc. 114 (1992) 4878. (e) K.-W. Kim, M.G. Kanatzidis, Inorg. Chem. 32 (1993) 4161. (f) J.-H. Chou, M.G. Kanatzidis, Inorg. Chem. 33 (1994) 1001, 5372. (g) J.-H. Chou, M.G. Kanatzidis, Chem. Mater. 7 (1995) 5. (h) J.-H. Chou, M.G. Kanatzidis, J. Solid State Chem. 123 (1996) 115. (i) J.-H. Chou, J.A. Hanko, M.G. Kanatzidis, Inorg. Chem. 36 (1996) 4.

[8] (a) A. Müller, V. Wittenben, E. Krickemeyer, H. Bögge, M. Lemke, Z. Anorg. Allg. Chem. 605 (1991) 175. (b) N.S. Hartig, P.K. Dorhout, S.M. Miller, J. Solid State Chem. 113 (1994) 88. (c) C.C. Raymond, P.K. Dorhout, S.M. Miller, Inorg. Chem. 33 (1994) 2703. (d) C.C. Raymond, P.K. Dorhout, S.M. Miller, Z. Kristallogr. 210 (1995) 776. (e) C.C. Raymond, P.K. Dorhout, S.M. Miller, ibid. 210 (1995) 775. (f) R.A. Stevens, C.C. Raymond, P.K. Dorhout, Angew. Chem. Int. Ed. Engl. 34 (1995) 2509.
[9] (a) W.S. Sheldrick, B. Schaaf, Z. Naturforsch. Teil B 49 (1994) 993. (b) W.S. Sheldrick, B. Schaaf, Angew. Chem. Int. Ed. Engl. 34 (1995) 450. (c) W.S. Sheldrick, M. Wachhold, Chem. Commun. (1996) 607.
[10] (a) W.S. Sheldrick, H.-J. Häusler, Z. Anorg. Allg. Chem. 557 (1988) 98, 105. (a) W.S. Sheldrick, H.-J. Häusler, ibid. 561 (1988) 139, 149. (c) W.S. Sheldrick, Z. Naturforsch. Teil B, 43 (1988) 249. (d) W.S. Sheldrick, H.G., Braunbeck, ibid. 44 (1989) 851; 45 (1990) 1643. (e) W.S. Sheldrick, H.G., Braunbeck, Z. Naturforsch. Teil B, 47 (1992) 151. (f) W.S. Sheldrick, B. Schaaf, Z. Naturforsch. Teil B., 49 (1994) 57; 49 (1995) 655.
[11] (a) H.A. Graf, H. Schäfer, Z. Anorg. Allg. Chem. 414 (1975) 211. (b) G. Dittmar, H. Schäfer, Z. Naturforsch. Teil B, 32 (1977) 1346. (c) A.S. Kanichtschewa, J.N. Mikhajilov, V.B. Lazarev, N.A. Moschchalkova, Dokl. Akad. Nauk. 252 (1980) 872. (d) B. Eisenmann, H. Schwerer, H. Schäfer, Mater. Res. Bull. 18 (1983) 383. (e) C. Brinkmann, B. Eisenmann, H. Schäfer, ibid. 20 (1985) 299.
[12] (a) G. Dittmar, H. Schäfer, Z. Anorg. Allg. Chem. 437 (1977) 183. (b) K. Volk, P. Bickert, R. Kolmer, H. Shcäfer, Z. Naturforsch. Teil B. 34 (1979) 380. (c) R.L. Bedard, S.T. Wilson, L.D. Vail, J.M. Bennett, E.M. Flanigen, in: P.A. Jacobs, R.A.v. Santen (Eds.), Zeolites: Facts, Figures, Future. Proceedings of the 8th International Zeolite Conference, Elsevier, Amsterdam, 1989, p. 375. (d) O.M. Yaghi, Z. Sun, D.A. Richardson, T.L. Groy, J. Am. Chem. 116 (1994) 807. (e) O. Achak, J.Y. Pivan, M. Maunaye, M. Loüer, D. Loüer, J. Solid State Chem. 121 (1996) 473.
[13] (a) J.B. Parise, J. Chem. Soc. Chem. Commun. (1985) 606. (b) J.B. Parise, Science 251 (1991) 293. (c) J.B. Parise, Y. Ko, Chem. Mater. 4 (1992) 1446. (d) K. Tan, A. Darovsky, J.B. Parise, J. Am. Chem. Soc. 117 (1995) 7039. (e) K. Tan, Y. Ko, J.B. Parise, A. Darovsky, Chem. Mater. 8 (1996) 448. (f) K. Tan, Y. Ko, J.B. Parise, J.-H. Park, A. Darovsky, ibid. 8 (1996) 2510.
[14] (a) Ref. [7f,g]. (b) H.-O. Stephan, M.G. Kanatzidis, J. Am. Chem. Soc. 118 (1996) 12226. (c) H.-O. Stephan, M.G. Kanatzidis, Inorg. Chem. 36 (1997) 6050.
[15] (a) H. Schäfer, B. Eisenmann, W.Müller, Angew. Chem. Int. Ed. Engl. 12 (1973) 694. (b) Ref. [1c]. (c) H. Schäfer, Annu. Rev. Mater. Sci. 15 (1985) 1. (d) P. Böttcher, Angew. Chem. Int. Ed. Engl. 27 (1988) 759.
[16] H. Jacobs, D. Schmidt, in: E. Kaldis (Ed.), Current Topics in Materials Science, Lausanne, North Holland, 1982.
[17] Lange's Handbook of Chemistry, p. 1.199, 5.105, 6.139.
[18] P.T. Wood, W.T. Pennington, J.W. Kolis, J. Am. Chem. Soc. 114 (1992) 9233.
[19] P.T. Wood, W.T. Pennington, J.W. Kolis, J. Chem. Soc. Chem. Commun. (1993) 235.
[20] P.T. Wood, W.T. Pennington, J.W. Kolis, Inorg. Chem. 33 (1994) 1556.
[21] J.E. Jerome, P.T. Wood, W.T. Pennington, J.W. Kolis, Inorg. Chem. 33 (1994) 1733.
[22] J. Li, B.G. Rafferty, S. Mulley, D.M. Proserpio, Inorg. Chem. 34 (1995) 6417.
[23] G.L Schimek, W.T. Pennington, J.W. Kolis, J. Solid State Chem. 123 (1996) 277.
[24] P.T. Wood, G.L Schimek, J.W. Kolis, Chem. Mater. 8 (1996) 721.
[25] D.M. Young, G. Schimek, J.W. Kolis, Inorg. Chem. 35 (1996) 7620.
[26] J. Li, Z. Chen, T.J. Emge, D.M. Proserpio, Inorg. Chem. 36 (1997) 1437.
[27] J. Li, Z. Chen, K.-C. Lam, S. Mulley, D.M. Proserpio, Inorg. Chem. 36 (1997) 684.
[28] J. Li, Z. Chen, J.L. Kelley, D.M. Proserpio, in: Solid State Chemistry of Inorganic Materials, ISBN: 1-55899-357-6, Vol. 453, 1997, pp. 29–34.
[29] J. Li, Z. Chen, X.-X. Wang, D.M. Proserpio, J. Alloys Comp. 262–263 (1997) 28.
[30] G.L. Schimek, J.W. Kolis, Chem. Mater. 9 (1997) 2776.
[31] G.L. Schimek, J.W. Kolis, Inorg. Chem. 36 (1997) 1689.

[32] T.K. Whittingham, Z. Chen, J. Li, D.M. Proserpio, Bull. N. J. Acad. Sci. 42 (1998) 11.
[33] Z. Chen, J. Li, T.J. Emge, T. Yuen, D.M. Proserpio, Inorg. Chim. Acta. 273 (1998) 310.
[34] J. Li, Z. Chen, F. Chen, D.M. Proserpio, Inorg. Chim. Acta. 273 (1998) 255.
[35] M.R. Girard, J. Li, D.M. Proserpio, Main Group Metal Chem. 21 (1998) 231.
[36] Z. Chen, R.E. Dilks, R.-J. Wang, J.Y. Lu, J. Li, Chem. Mater. 10 (1998) 3184.
[37] (a) J. Li, Z. Chen, R.-J. Wang, J.Y. Lu, J. Solid State Chem. 140 (1998) 149. (b) Z. Chen, R.-J. Wang, J. Li, J. Solid State Chem., in press.
[38] K.-C. Lam, Z. Chen, R.-J. Wang, J. Li, unpublished results.
[39] Z. Chen, R.-J. Wang, J. Li, Chem. Mater., submitted.
[40] Z. Chen, R.-J. Wang, J. Li, Chem. Mater., submitted.
[41] A.K. Cheetham, P. Day (Eds.), Solid State Chemistry: Compounds, Clarendon Press, Oxford, 1992.
[42] M.A. Ansari, J.M. McConnachie, J.A. Ibers, Acct. Chem. Res. 26 (1993) 574.
[43] R.C. Burns, J.D. Corbett, Inorg. Chem. 20 (1981) 4433.
[44] R.C. Haushalter, Angew. Chem, Int. Ed. Engl. 24 (1985) 433.
[45] S.S. Dhingra, C.J. Warren, R.C. Haushalter, A.B. Bocarsly, Chem. Mater. 6 (1994) 2382.
[46] M.G. Kanatzidis, Comments Inorg. Chem. 10 (1990) 161.
[47] J.C. Bollinger, L.C. Roof, D.M. Smith, J.M. McConnachie, J.A. Ibers, Inorg. Chem. 34 (1995) 1430.
[48] J.M. McConnachie, M.A. Ansari, J.C. Bollinger, J.A. Ibers, Inorg. Chem. 32 (1993) 3201.
[49] U. Müller, C. Grabe, B. Neumüller, B. Schreiner, K. Dehnicke, Z. Anorg. Allg. Chem. 619 (1993) 500.
[50] K.-W. Kim, M.G. Kanatzidis, Inorg. Chim. Acta 224 (1994) 163.
[51] A. Bondi, J. Phys. Chem. 68 (1964) 441.
[52] N.W. Alcock, Adv. Inorg. Chem. 15 (1972) 1.
[53] B. Schreiner, K. Dehnicke, K. Maczek, D. Fenske, Z. Anorg. Allg. Chem. 619 (1993) 1414.
[54] Y. Saito, Inorganic Molecular Dissimmetry, Springer-Verlag, Berlin, 1979, pp. 56–59.
[55] E.R. Franke, H. Schäfer, Z. Naturforsch. Teil B 37 (1972) 1308.
[56] Y.-C. Hung, S.-J. Hwu, Acta Crystallogr. Sect C 49 (1993) 1588.
[57] S.S. Dhingra, C.J. Warren, R.C. Haushalter, A.B. Bocarsly, Chem. Mater. 6 (1994) 2376.
[58] D. Müller, G. Eulenberger, H. Hahn, Z. Anorg. Allg. Chem. 398 (1973) 207.
[59] W. Klee, H. Schäfer, Z. Anorg. Allg. Chem. 479 (1981) 125.
[60] (a) C.J. Warren, S.S. Dhingra, R.C. Haushalter, A.B. Bocarsly, J. Solid State Chem. 112 (1994) 340. (b) C.J. Warren, R.C. Haushalter, A.B. Bocarsly J. Alloys Comp. 229 (1995) 175.
[61] C.-W. Park, R.J. Salm, J. Ibers, Angew. Chem. Int. Ed. Engl. 34 (1995) 1879.
[62] P.H. Smith, K.N. Raymond, Inorg. Chem. 24 (1985) 3469.
[63] (b) B.A. Katz, C.E. Strouse, Inorg. Chem. 19 (1980) 658. (b) B.A. Katz, C.E. Strouse, J. Am. Chem. Soc. 101 (1979) 6214.
[64] See for example: (a) J. Cernak, Chomic, M. Dunaj-Jurco, C. Kappenstein, Inorg. Chim. Acta 85 (1984) 219. (b) J. Emsley, M. Arif, P.A. Bates, M.B. Hursthouse, Inorg. Chim. Acta 165 (1989) 191.
[65] The crystal chemical classification used for silicate and other tetrahedral compounds is adopted here: the periodicity of a single chain is defined as the number of polyhedra within one repeating unit of the linear part of the chain. To denote a silicate anion according to its periodicity, one uses the terms einer, zweier, dreier etc. for periodicity 1, 2, 3. These terms are derived from the German numerals, eins, zwei, drei··· by adding a suffix 'er'. See: F. Liebau, Structural Chemistry of Silicates; Springer, Berlin, 1985.
[66] S.S. Dhingra, M.G. Kanatzidis, Inorg. Chem. 32 (1995) 1350.
[67] See (a) Ref. [65], page 80. (b) J. Li, Y.Y. Liszewski, L.A. MacAdams, F. Chen, S. Mulley, D.M. Proserpio, Chem. Mater. 8 (1996) 598.
[68] L.-H. Liao, J. Li, M.G. Kanatzidis, Inorg. Chem. 34 (1995) 2658 and references therein.
[69] V.P. Fedin, H. Imoto, T. Saito, W. McFarlane, A.G. Sykes, Inorg. Chem. 34 (1995) 5097.
[70] (a) L.E. Bogan Jr., T.B. Rauchfuss, A.L. Rheingold, Inorg. Chem. 24 (1985) 3720. (b) A. Seigneurin, T. Makani, D.J. Jones, J. Roziere, J. Chem. Soc. Dalton Trans. (1987) 2111.
[71] B. Eisenmann, J. Hansa, Z. Kristallogr. 203 (1993) 299.

[72] W.S. Sheldrick, B. Schaaf, Z. Anorg. Allg. Chem. 620 (1994) 1041.
[73] S. Jaulmes, P. Houenou, Mater. Res. Bull. 15 (1980) 911.
[74] M.A. Pell, J.A. Ibers, Inorg. Chem. 35 (1996) 4559.
[75] B. Eisenmann, R. Zagler, Z. Naturforsch. Teil B 44 (1989) 249.
[76] P. Böttcher, H. Buchkremer-Hermanns, Z. Naturforsch. Teil B 42 (1987) 267.
[77] H. Buchkremer-Hermanns, P. Böttcher, J. Less-Common Met. 137 (1988) 1.
[78] R.M. Imamov, Z.G. Pinsker, A.I. Ivchenko, Z. Kristallogr. 9 (1964) 853.
[79] A. Pfitzner, Z. Anorg. Allg. Chem. 621 (1995) 685.
[80] A. Pfitzner, Z. Kristallogr. 209 (1994) 685.
[81] J. Li, H.-Y. Guo, R.A. Yglesias, T.J. Emge, Chem. Mater. 7 (1995) 599.
[82] H.R. Heulings, J. Li, D.M. Proserpio, Main Group Met, Chem. 21 (1998) 225.
[83] Z. Ban, M. Sikirica, Acta Crystallogr. 18 (1965) 594.
[84] W. Bensch, P. Duerichen, C. Weidlich, Z. Kristallogr. 211 (1996) 932.
[85] M.G. Kanatzidis, J.-H. Chou, J. Solid State Chem. 127 (1996) 186.
[86] W. Bensch, P. Duerichen, Z. Kristallogr. 212 (1997) 97.
[87] K.O. Klepp, C. Weithaler, Z. Natursch. Teil B. 50 (1995) 1791.